SRI International

Final Report (Rev.)—Task 6.0.2 • January 1990

OBSERVATION OF NEUROMAGNETIC FIELDS IN RESPONSE TO REMOTE STIMULI

Prepared by: Edwin C. May
Wanda W. Luke
Virginia V. Trask
Thane J. Frivold

SG1J

Prepared for: [redacted]
Contracting Officer's Technical Representative

SRI Project 1291

Approved by: Murray J.Baron, Director
Geoscience and Engineering Center

333 Ravenswood Avenue • Menlo Park, CA 94025-3493 • (415) 326-6200 • FAX: (415) 326-5512 • Telex: 334486

Approved For Release 2000/08/08 : CIA-RDP96-00789R002200630001-8

ABSTRACT

We have conducted a conceptual replication of an SRI/Langley Porter study in which a single subject's central nervous system (CNS) responded to a remote, and isolated flashing light. The CNS activity of eight remote viewers was monitored by a seven-channel magnetoencephalograph (MEG). Visual stimuli were randomly presented to an isolated individual who acted as a "sender" while MEG data were collected from a viewer (receiver). The stimuli were 5-cm square, linear, vertical, sinusoidal gratings lasting 100 ms (remote stimuli). Time markers were randomly inserted into the data stream as control points (pseudo stimuli). The dependent variable was the root-mean-square (RMS) average phase shift of the dominant alpha frequency. Using a Monte Carlo technique to estimate p-values, we observed significant (combined across all viewers) RMS phase shifts resulting from the remote stimuli ($Z_s = 1.99, p \leq 0.024$, *effect size* $= 0.599$). Similarly, the combined statistic for the pseudo stimuli was also significant ($Z_s = 2.92, p \leq 0.002$, *effect size* $= 0.924$). The phase shifts from the remote and the pseudo stimuli are independently *not* characteristic of the data at large. This result was unexpected, and suggests that we may have observed a CNS response to an unintended stimulus (i.e., electromagnetic interference, EMI, from the computing hardware). However, in the SRI/Langley Porter study, EMI had been eliminated, thus, it remains possible that the CNS changes resulted from an anomalous form of information transfer.

TABLE OF CONTENTS

LIST OF TABLES

LIST OF FIGURES

combination of electrical signals and chemical interactions. It is beyond the scope of this report to describe the cellular physiology involved, but is sufficient to say that this activity produces magnetic fields (predominantly dipole) that can be sensed externally.

The sensing device of a MEG is a cryogenic superconducting quantum interference device (SQUID) coupled with a gradiometer. SQUIDs currently being used are cooled by liquid helium. At a few degrees above absolute zero, an electrical current can flow through a superconductor with no applied voltage. The material of the SQUID consists of superconducting loops with two sections of thin insulating material connecting them (Josephson Junctions). This configuration is referred to as a DC SQUID. Some electrons can tunnel through this insulation. The presence of a weak magnetic field produces a phase difference for the wave function of the magnetic field [and] produces a phase difference for the wave function of the electrons across this barrier. The resulting interference pattern produced by the two different wave functions on each side of the barrier can be used to indicate the strength of these extremely weak magnetic fields.

The neuronal magnetic fields from the human brain are only about 10^{-13} tesla, while the earth's magnetic field is 10^{-4} tesla and normal urban noise is about 10^{-7} tesla. Care must be taken, therefore, to assure that the signal-to-noise ratio is favorable. This has been taken into consideration by the manufacturer of MEG equipment (BTi of San Diego, California), who has designed highly shielded sensors that use a second-order coupled gradiometer to reduce the environmental noise by about 10^6. The use of an aluminum and μ-metal magnetically shielded room can further reduce the noise by a factor of 10^3. If used together, these two precautionary measures can reduce the ambient noise by a factor of about 10^9—equivalent to the internal SQUID noise.

Because a MEG responds best to neuronal currents that are parallel to the skull (i.e., currents producing magnetic fields oriented tangentially to the skull), neuronal currents perpendicular to the skull may be missed. In reality, however, few neuronal electrical currents are exactly perpendicular to the skull, so some tangential component is almost always available to the SQUID.

Searching for a closely packed group of neurons can be a slow and tedious process. Due to technological restraints, a maximum of seven sensors can be used simultaneously to gather MEG measurements. Sensors on a seven-channel MEG are located on a 2-cm equilateral triangular grid forming the center and vertices of a regular hexagon. A subject wears a spandex cap with grid marks lined up with his nasion, inion, and earlobes to serve as a head-centered coordinate system. To identify the location of a neuronal-equivalent current dipole, many measurements have to be taken. Isocontour maps of field strength are used to represent the amplitude and polarity distribution of the magnetic fields. A least-squares procedure is applied to the observed fields to estimate the location of neuronal sources and orientation of the equivalent current dipole.[8] The estimated location of the neuronal source can then be identified anatomically with a magnetic resonance image scan of the head. Developments in technology may soon allow for enough channels to cover the whole head at once, thereby reducing data collection time and increasing precision.

MEG technology is based on a cryogenic SQUID operating in liquid helium. Because the Dewar flask cannot exceed a 45-degree angle, subjects must lie prone beneath the apparatus. MEG sensors are not attached to the head, but are lowered into position over the skull; the subject cannot move his head during monitoring without disturbing the measurement. For these two reasons, MEG equipment is not suited for long-term monitoring of a subject. These problems may be solved in the near future as new technology, such as high-temperature SQUIDs, develops.

A response from the MEG is a complex waveform consisting of a series of negative and positive peaks or components. Specific components of this waveform can be correlated with perceptual and cognitive processes. The most commonly observed response to a visual or auditory stimulus, for example, is a large component occurring approximately 100 ms after the onset of the stimulus. One hundred milliseconds appears to be the average latency period between stimulus and the first correlated neuronal activation in the brain.[8]

The earlier EEG technology measures electric potential, or event-related potentials (ERPs) produced by the electrical activity of the brain. A MEG measures the magnetic fields, or event-related fields (ERFs) produced by the electrical activity of specific groups of active neurons in the cortex. An EEG and a MEG, therefore, reveal different aspects of the electrical activity of the

brain and are often used as complementary technologies. In some areas, however, the MEG technique has definite advantages over the EEG:

(1) ERPs taken from the scalp provide little information regarding the precise three-dimensional distribution of the neuronal sites producing the electrical activity. Brain tissues of unknown electrical conductivity and thickness, individual variations in skull thickness and geometry, and proximity to openings in the skull all make obtaining such detailed information difficult. The same is not true when using a MEG. Neuronal magnetic fields can travel through brain tissues without being significantly altered; this property, coupled with the dipole model, results in high spatial resolution of the neuronal activity.

(2) EEG procedures are occasionally costly and can be invasive: EEG electrodes must be attached directly to the skull or to the brain of the subject, whereas MEG sensors are extracranial and are simply lowered into position against the skull.

(3) There is much controversy over the appropriate reference electrode in EEG work (a reference electrode is required with electric potential measurements, because only differences in electric potential are measured). There is no such problem with a MEG, because the measurement of magnetic fields is absolute.

II METHODS OF APPROACH

Our goal was to conduct a conceptual replication of the earlier SRI/Langley Porter experiments. Our basic hypothesis is that a viewer's CNS would respond to a remote light stimulus.

1. General Description

Using a seven-sensor MEG in a shielded room, we investigated the occipital-cortex neuronal magnetic activity that might occur in response to a remote "visual" stimulus.

The following definitions may be helpful:

- Viewer—An individual who attempts extrasensorimotor communication with the environment (e.g., the perception of remote stimuli).
- Direct Stimuli (DS)—Visual stimuli occurring within the normal visual sensory channels.
- Sender—An individual who, while receiving direct stimuli, acts as a putative transmitter to a remote individual (i.e., viewer) who is attempting to receive the same information via extrasensorimotor communication.
- Remote Stimuli (RS)—Visual stimuli occurring outside the normal range of known sensory channels.
- Pseudo Stimuli (PS)—A time marker in the data stream with no associated stimuli.

In this report, a direct stimulus to the sender is also considered as a remote stimulus to the viewer.

2. Protocol

2.1 General Considerations

To begin a session, a sender is isolated in a room while a viewer is monitored by a MEG in a shielded room about 40 m away. Only the sender is presented with a number of direct visual stimuli at random intervals within a 120-second period, the length of one run. One session usually consists of 10 runs.

2.1.1 Viewers

Eight viewers were selected for this experiment. Four were known to be good remote viewers, and four were staff members with unknown viewing ability. Each viewer contributed a minimum of one and a maximum of three independent sessions.

2.1.2 Senders

The senders in all sessions were either various staff members who were well known to the viewers or they were spouses.

2.1.3 Dependent Variable

The dependent variable is the root-mean-square (RMS) phase shift of the primary alpha activity as a result averaged over all RS.

2.2 Specific Protocol Details

2.2.1 Stimuli

Remote stimuli consisted of a standard video encoded blank screen with a 5-cm square, linear, vertical, sinusoidal grating lasting about 100 ms. These stimuli (DS to the sender) subtended 2 degrees in the lower left visual field of the sender. This was maintained by asking the sender to focus his visual attention on a permanent mark on the monitor. During the experiments described in this report, no attempt was made to monitor the sender in any way. Pseudo stimuli consisted of the blank screen without the superimposed grating, and were included as a putative within-run control.

2.2.2 Run Timing

Figure 1 shows a schematic timing diagram for one run. No two stimuli of any type were allowed to occur within a 3-second period of each other. A stimulus may occur, however, any time within a 4.5-second window thereafter. The sender was

presented with a minimum of 9 and a maximum of 15 DS occurring at random intervals within a 120-second period. In all but the first session, a random number of pseudo stimuli (i.e., random time markers with no concomitant stimuli—PS) were added as a within-run control. A viewer was never presented with direct stimuli except in locating the maximal response to the visual areas (see Section II.2.2.4).

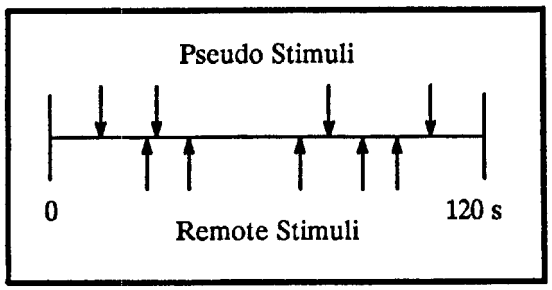

Figure 1 Schematic Timing Protocol—Single Run

2.2.3 Instructions to Viewers

In all sessions, the viewers were completely informed about the details of the experiments. Prior to their placement on the MEG table, they were shown the location of the RS display monitor, and were instructed to place their attention upon it or the sender during the session.

For some sessions, the viewer was instructed to press a fiber-optic-coupled button when he felt that he perceived stimuli. Each button press was marked in the data record. Button pressing was retained in this protocol as part of the conceptual replication.

2.2.4 Sensor-array Placement and Calibration

We selected the location for the sensor array by optimizing the viewer's response to direct visual stimuli. Inherent in this choice is an assumption that may not be valid: namely, that neurons participating in a reaction to RS are the same as those that respond to DS. The sensor locations were then marked on an acetate transparency to allow for accurate repositioning of the sensors in later sessions. One such placement (right occipital—minus centimeters from the inion indicate the right hemisphere) is shown for viewer 002 in Figure 2. It should be noted that MEG sensor placements do not necessarily correspond to conventional EEG electrode placement.

For a calibration, the viewer was fitted with a spandex cap with grid marks aligned with his inion, nasion, and earlobes (i.e, head-centered coordinate system). The viewer was then placed as comfortably as possible on an observation table beneath the MEG. He must lie face down and look though a hole in the table to view the DS via a system of mirrors. These stimuli were displayed by a projector located outside the entrance to the shielded room. The sensors of the MEG were lowered from above to touch his head over the right occipital lobe. In this configuration, the sensor array was moved at the end of 30 DS to a position that optimized his response to the DS. Once found, the array position was marked on the cap for subsequent repositioning.

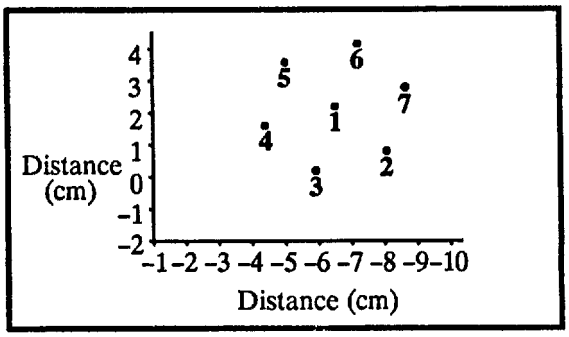

Figure 2 Sensor Position Relative to the Inion (0,0) for Viewer 002

2.2.5 Sequence of Events for a Session

The following is the schedule of events for a session:

- Collect approximately 10 minutes of background data with no viewer or sender present and the MEG in full operation.
- Isolate the sender with the stimulus display device.
- With the viewer on the table, position the sensor array at the calibration point.
- At time = 0, start the monitoring of data with computer-generated trigger. Data are collected the entire 120 seconds at a rate of 200 samples per second.
- At time < 120 seconds, present 9 to 15 remote and 9 to 15 PS to the sender.
- At time > 120 seconds, allow the viewer to relax for about 2 to 5 minutes without leaving the table. This break generally consists of the sender entering the shielded room to engage the viewer in conversation.

- Collect nine additional runs with the same procedure while the viewer remains positioned on the table under the MEG.

3. Data Analyses

If our initial assumption about sensor positioning is true, and if the earlier results are replicated, we expect to see a change in alpha production as a result of the RS. We might also expect an evoked response similar to visual ERFs. Figure 3 is an idealized illustration of these expected results in the time-series data. Times less than zero are prestimulus; times greater than zero are poststimulus. The stimulus lasts 100 ms.

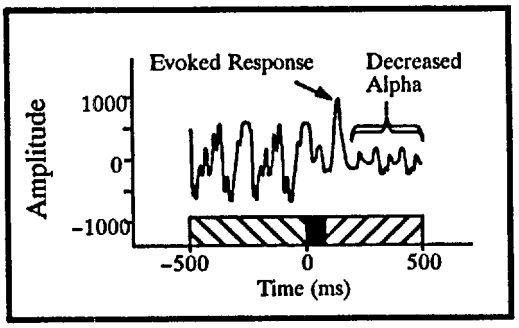

Figure 3 Idealized Results for a Single Stimulus

For each session, the following was computed for each RS and PS, respectively:

(1) Five hundred ms of pre- and post-stimulus time-series data were separately detrended and filtered (40 Hz lowpass).

(2) The power spectrum was computed for each 500-ms pre- and post-stimulus period.

(3) The relative phase change of the dominant alpha frequency from pre- to post-stimulus period was computed as the arctangent of the ratio of the imaginary and real component of the transfer function. The transfer function is defined as the ratio of the FFT of the post-stimulus period divided by the FFT of the pre-stimulus period.

(4) One thousand ms of time-series data (i.e., 500 ms pre- and post-stimulus) was separately detrended and filtered (40 Hz lowpass).

In addition, the following averages were computed across all RS and PS, respectively:

(5) The average power pre- and post-stimulus.

(6) The root-mean-square (RMS) average phase shift.

(7) The 1000-ms time average of the pre- and post-stimulus periods taken as a single record.

(8) The "power spectra" of the pre- and post-stimulus time averages were computed. (We recognize that a power spectrum of a time average is not an accurate representation of the average power spectrum, however it is an indicator of phase shift.)

4. Monte Carlo Calculations

The analysis of CNS activity has always been problematic, because alpha bursts lasting from 0.1 to a few seconds occur at random intervals. From a statistical point of view, the data fail to satisfy at least two underlying assumptions of the usual statistical methods (e.g., ANOVA and MANOVA). Most standard statistical tests assume that all samples of the data are independent. MANOVA can be configured to remove this particular assumption, nonetheless, it and the other tests assume that the process under study is stationary; that is, whatever the statistical properties are, they remain constant over time. In other words, the measured properties should not depend upon when the activity is sampled. CNS time series data do not satisfy either of these assumptions.

To avoid these difficulties, and to obtain probability estimates of the observed RMS phase shifts, we adopted a simple Monte Carlo approach. In the usual statistical analysis, the phase shift is compared to an ideal distribution, or its likelihood of occurrence is computed using some nonparametric technique. Both techniques attempt to determine the degree to which the observed phase shift is exceptional, given the universal set of all possible data. The Monte Carlo method that we used, however, can only determine the degree to which the observed phase shift is exceptional, given the available data sample. Thus, a new Monte Carlo estimate must be computed for each individual data set.

The general Monte Carlo procedure is as follows:

(1) Using the same timing algorithm to create the original RS, generate N sets of M stimuli, where M is the number of original RS.

(2) For each pass ($1...N$), compute the RMS phase shift averaged over M remote stimuli.

(3) Sort the resulting N values to form the RMS phase shift distribution in the given data sample.

(4) Compute the probability that the observed value would be as large (or larger), given a repeated random sample of the data. Note that this p–value is *not* the probability that the measure is as large, given a different data sample.

We have used this technique to compute p–values for the RMS phase shifts throughout this report.

III RESULTS

Eight viewers (002, 007, 009, 372, 374, 389, 454, and 531) from SRI International participated in the effort. Viewers 002, 009, 372, and 389 were experienced, with strong track records. Viewers 007, 374, and 531, had not previously participated in remote viewing experiments. Viewer 454 had participated in novice remote viewing training and has produced significant evidence of remote viewing ability.

1. Calculations

To illustrate the reduction of the raw data, we use the 25 September 1988 session from viewer 002.

Figure 4 shows the time average over all RS of the amplitude (femto Tesla) of the magnetic CNS activity of viewer 002's response to RS. The data from all seven sensors are displayed in a pattern that is similar to the physical sensor array. Each sensor is labeled in a highlighted box. The number of stimuli comprising the average (118) is shown in the key. The onset of the 100-ms stimulus is represented at *time = 0*, so negative time represents the pre-stimulus period and positive time represents the post-stimulus period. The total time period shown is 1 second. Because the stimuli are at random times relative to any uncorrelated CNS activity, averaging has reduced random single-stimulus amplitudes by $\sqrt{n}$ where n is the number of stimuli. Sensor 7 shows a clear change from a slow, regular alpha rhythm during the pre-stimulus period, to one of higher frequency, post-stimulus.

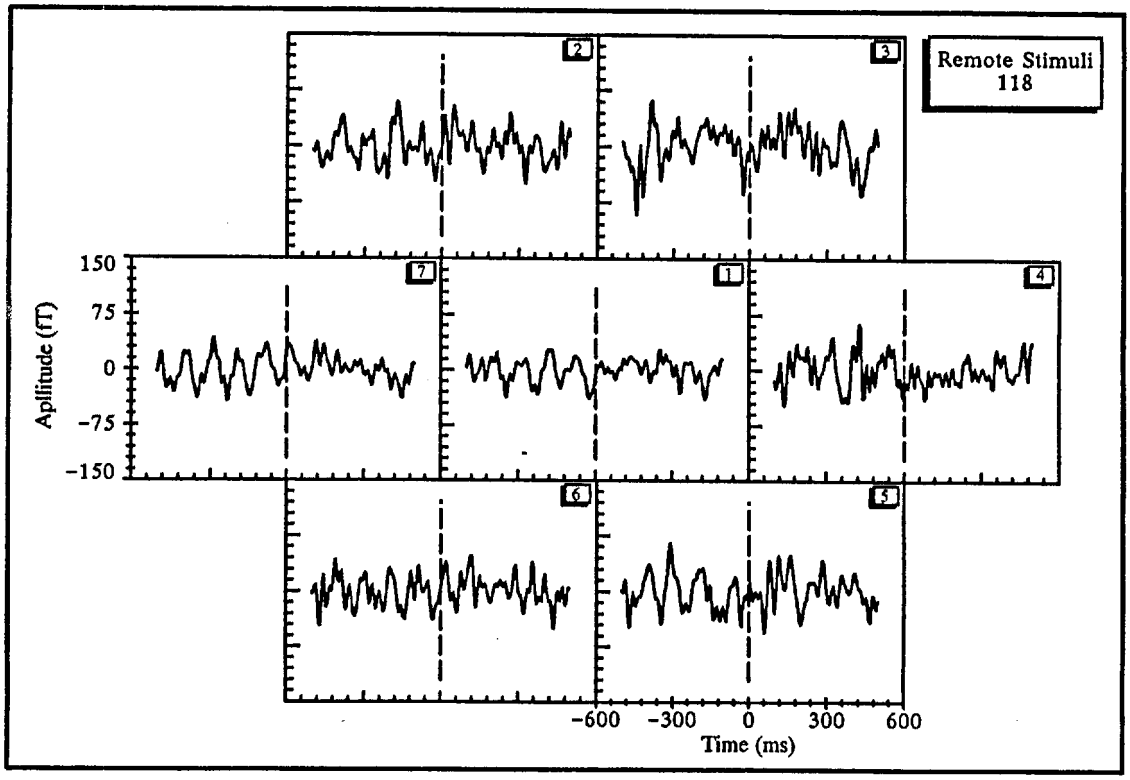

Figure 4 Viewer 2: Date 8/25/88: Session 1: Time Average

Figure 5 shows this change of alpha in the frequency domain. For each sensor, the power spectrum of its corresponding time series is displayed from 0 to 40 Hz. The power spectra are shown independently for the pre- and post-stimulus periods (separated by a dashed vertical line). Sensor 7 shows a strong 10-Hz peak pre-stimulus that vanishes post-stimulus Similar alpha reductions can be seen in all of the other six sensors.

The power spectrum of a time series average is *not* an indicator of the average power spectrum of the CNS activity, because time averages are phase sensitive and power spectra are not. Figure 6 illustrates this by showing the average power spectra (i.e., calculated on a stimulus-by-stimulus basis and then averaged) for the pre- and post-stimulus periods.

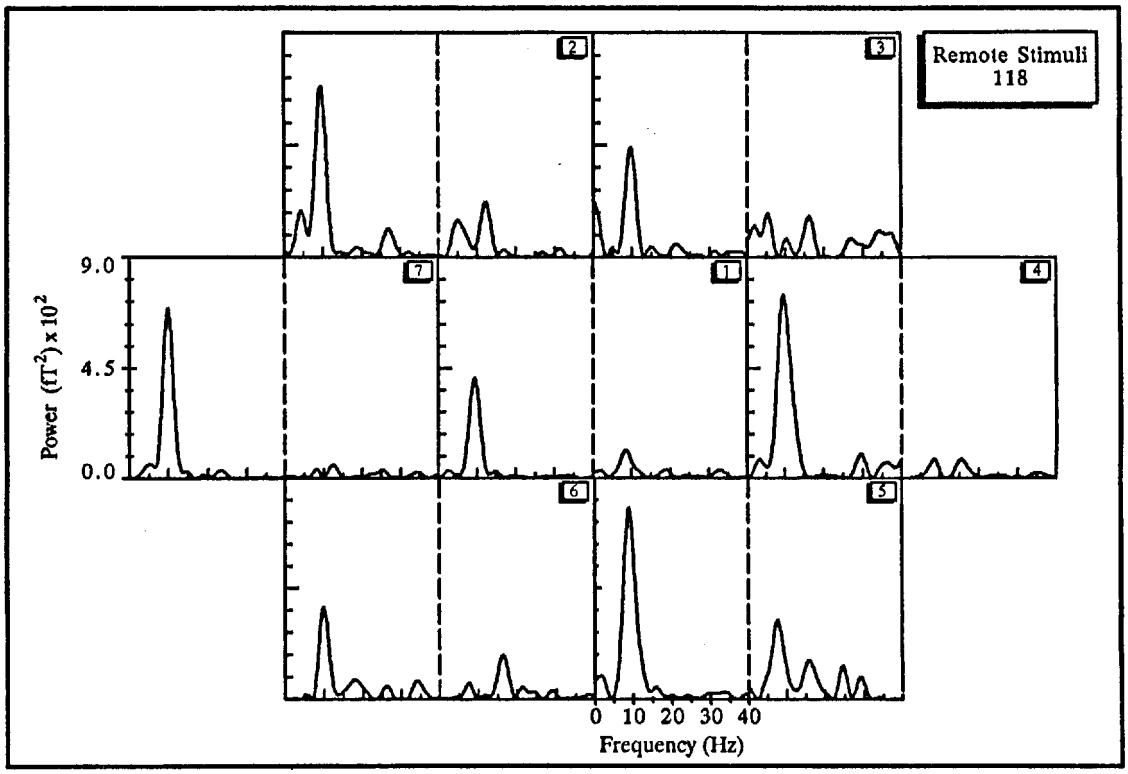

Figure 5 Viewer 2: Date 8/25/88: Session 1: Power of Time Average

Figure 7 shows the ratio of the post- to pre-stimulus power. A dashed horizontal line is shown to indicate a gain of 1 (i.e., no change across the stimulus boundary). In this example, there is little change of CNS power across the stimulus boundary throughout the frequency range.

Because a time average is sensitive to relative phase and a power spectrum is not, these data suggest that a relative phase shift occurs between pre- and post-stimulus periods. Figure 8 shows this relative RMS phase shift computed from 0 to 40 Hz for all sensors. As was the case for the time-series data, the RMS average was computed over $n = 118$ RS. In accordance with the protocol (Section II.3), the dependent variable was the RMS phase only at the dominant α-frequency.

At this point we are unable to determine if the variations seen in Figures 4 through 8 are meaningful. Toward that end, the identical quantities for the PS are shown in Figures 9 through 13. The "power" of the time averages for the remote stimuli differ markedly from those of the PS spectra (Figures 5 and 10).

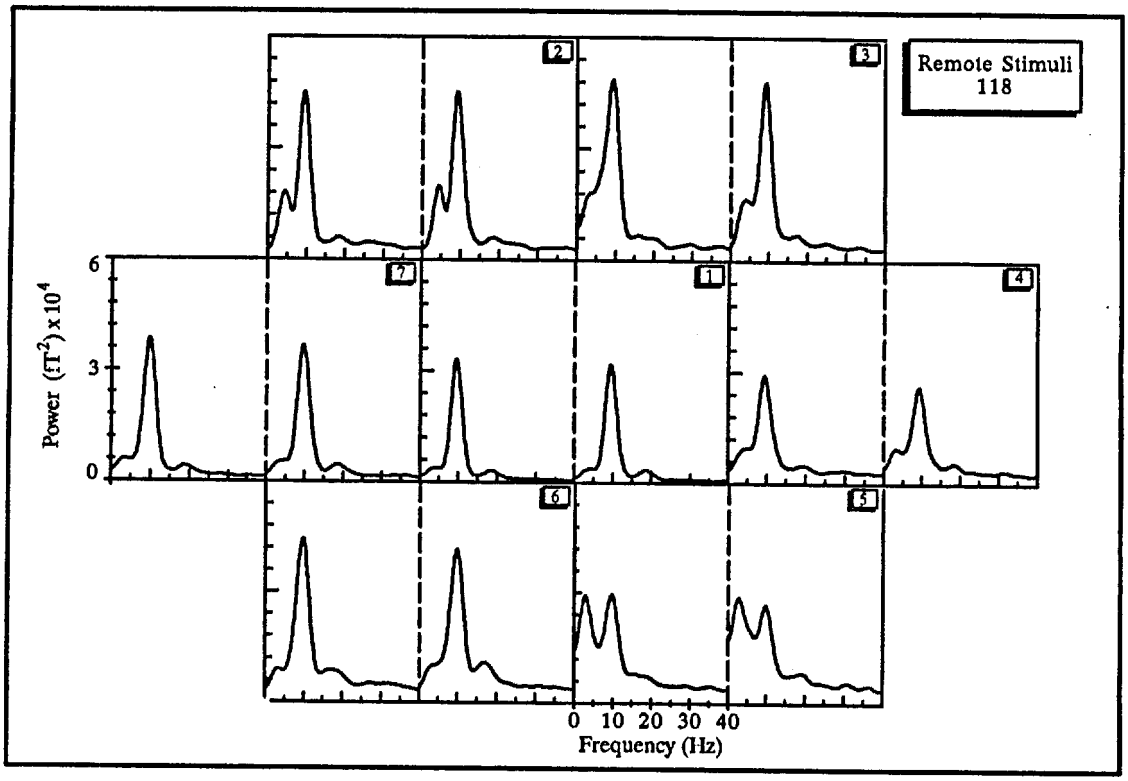

Figure 6 Viewer 2: Date 8/25/88: Session 1: Average Power

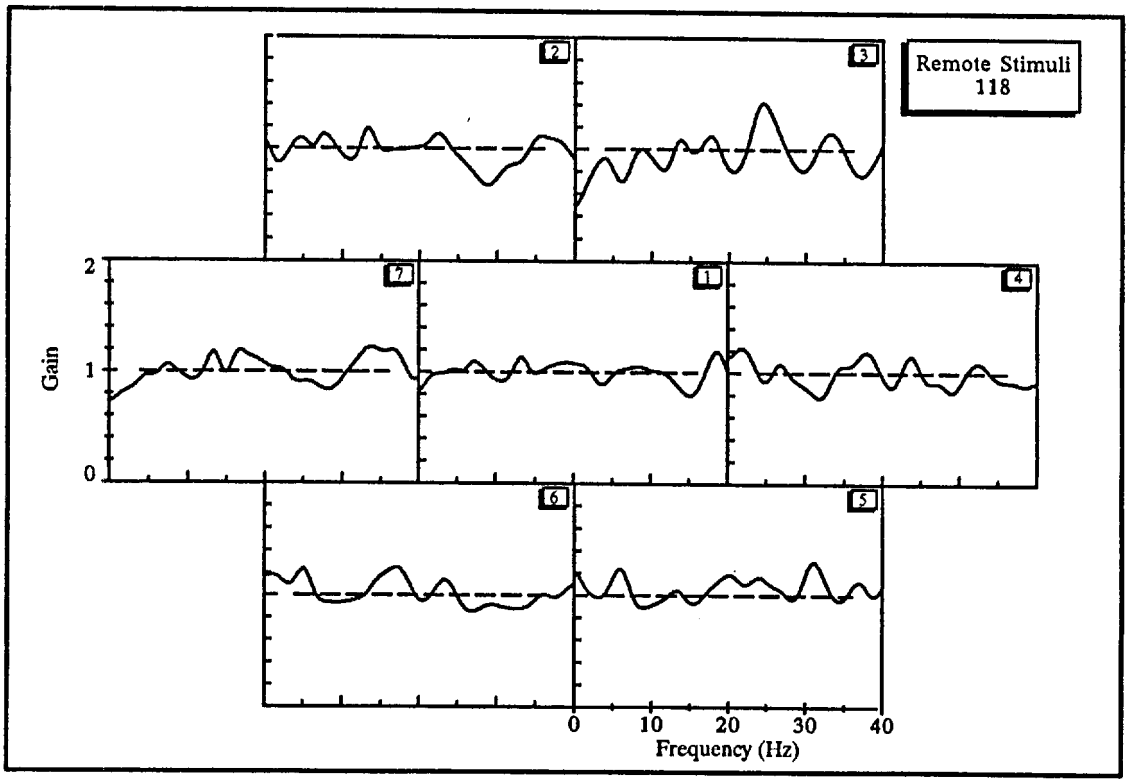

Figure 7 Viewer 2: Date 8/25/88: Session 1: Average Power Gain

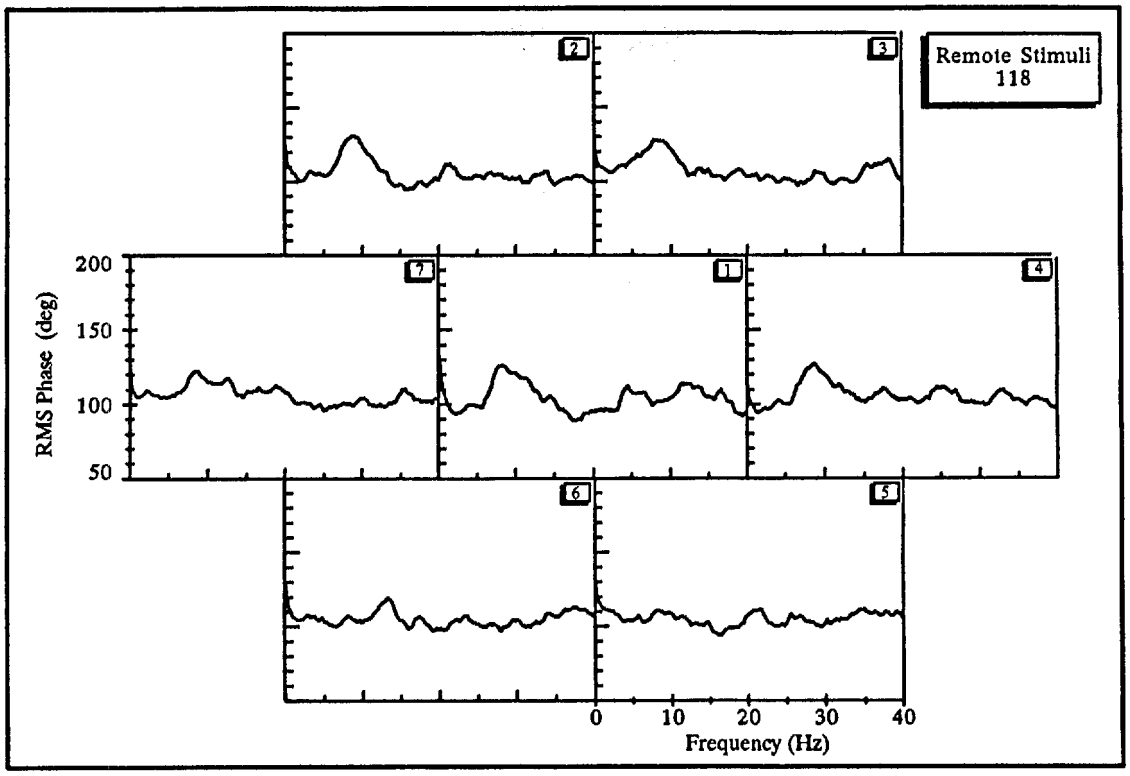

Figure 8 Viewer 2: Date 8/25/88: Session 1: RMS Phase

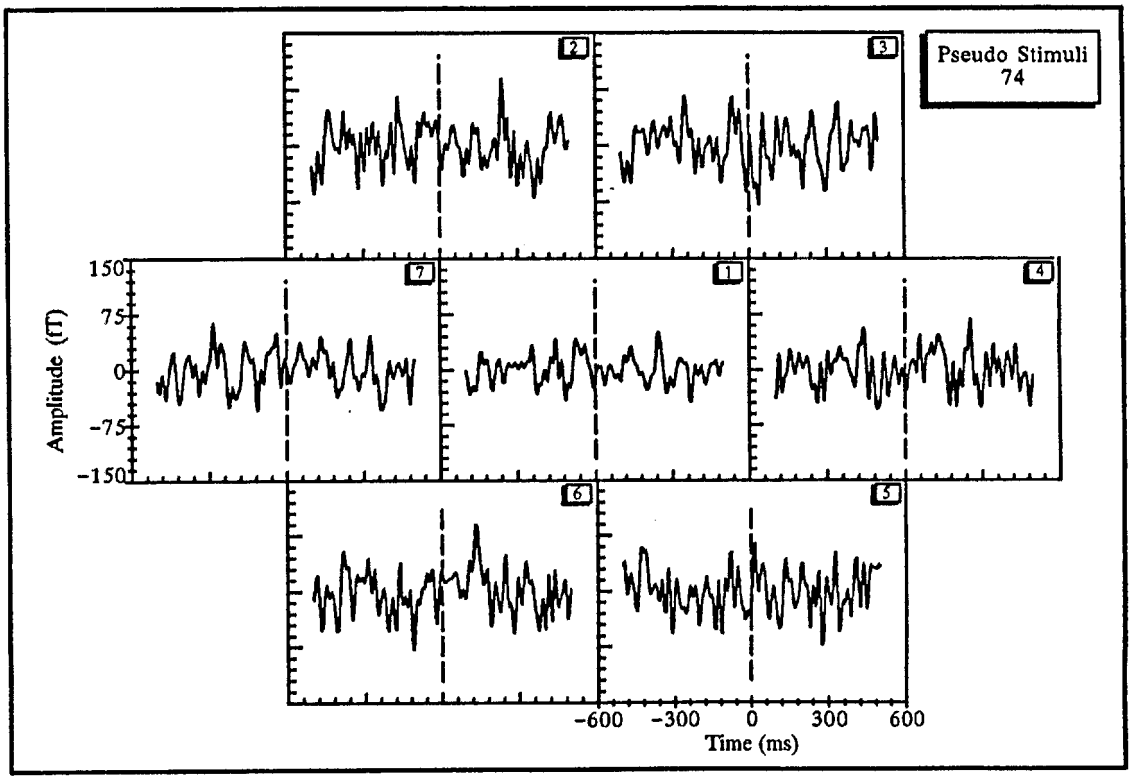

Figure 9 Viewer 2: Date 8/25/88: Session 1: Time Average

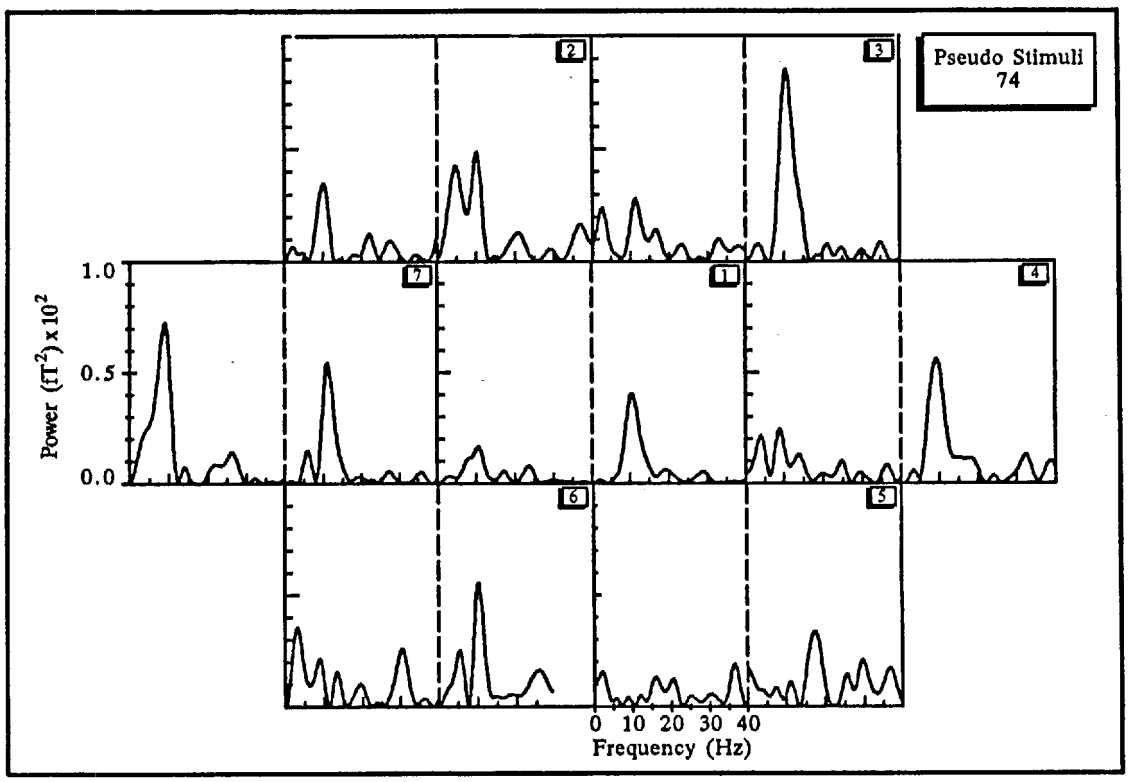

Figure 10 Viewer 2: Date 8/25/88: Session 1: Power of Time Average

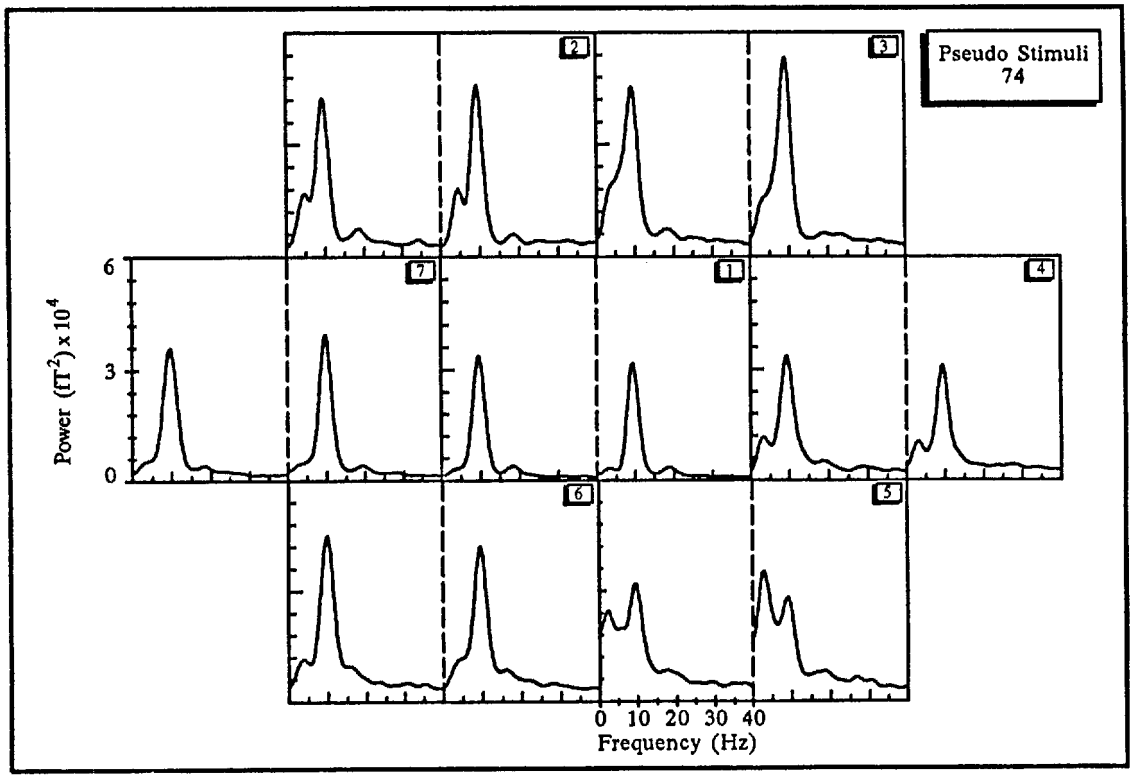

Figure 11 Viewer 2: Date 8/25/88: Session 1: Average Power

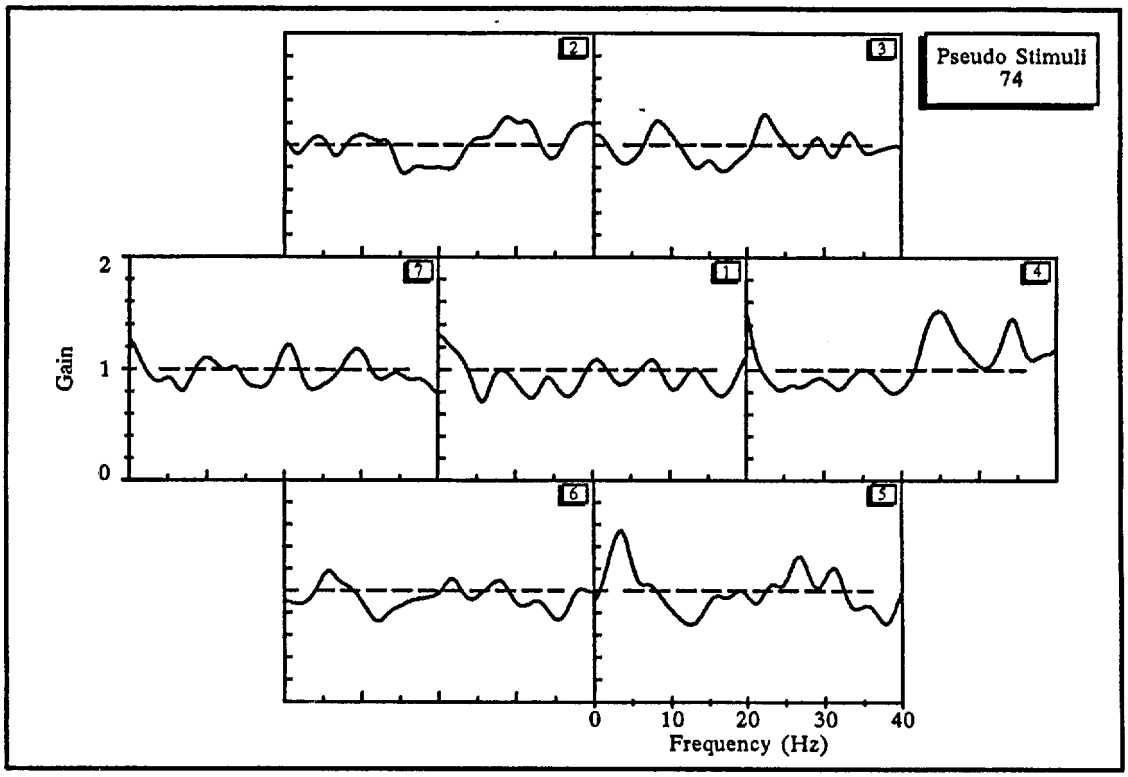

Figure 12 Viewer 2: Date 8/25/88: Session 1: Average Power Gain

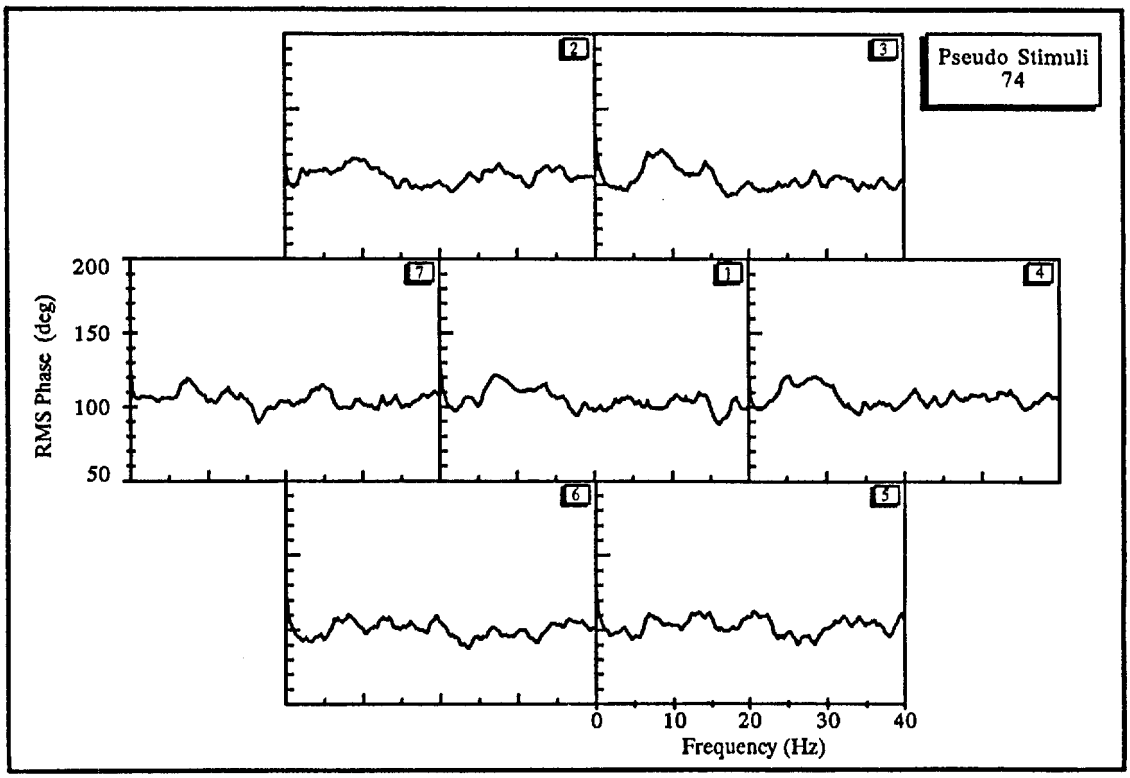

Figure 13 Viewer 2: Date 8/25/88: Session 1: RMS Phase

2. Monte Carlo Estimates of Significance

To determine if the changes that are seen qualitatively are exceptional, we analyzed the data by the Monte Carlo procedure outlined in Section II.4. We simulated the RS by generating 500 sets of Monte Carlo stimuli using the same random timing algorithm and number as in the original data. For each set, the RMS phase was calculated as described in Section II.3. The resulting 500 Monte Carlo RMS phases were sorted as a descending array, and the fraction of phases equal to or larger than the observed RS value was represented as a p–value. (The p–value is bounded on the low end by 1/500.) Figure 14 shows a histogram of one such Monte Carlo run, again using the data from viewer 002 as an example. The values of the RMS phase for the remote and pseudo stimuli are marked by vertical lines (see the key in Figure 14).

In accordance with the earlier study[6] in which we observed changes in alpha power, we established a single criterion for the selection of a sensor for analysis: the pre-stimulus average alpha power above background is larger than it is in any other sensor. Table 1 shows the viewer identification, date, sensor chosen for analysis, and the p–value (as defined above) for the RMS phase shift for the remote and pseudo stimuli, respectively.

The p–values shown in Table 1 are all single tailed (i.e., the area in the upper tail). Because the distribution of means is approximately normal, we have converted the empirical p–values to their respective two–tailed z–scores. If the p–value was less than 0.5, the z–score shown in Table 1 was computed from the inverse normal distribution assuming a p–value twice the one shown. If the p–value was more than 0.5, we subtracted it from 1.0, doubled the result, and computed the z–score as above. To test the null hypothesis that the combined RS phase shifts are characteristic of the data, we computed a standard Stouffer's Z (Z_s) for the 11 sessions shown in Table 1. There is statistical evidence that the data within $\pm$ 0.5 seconds of the RS are *not* characteristic of the data at large ($Z_s = 1.99, p \leq 0.024$, *effect size* = 0.599). Similarly, the combined statistic for the PS indicates that these data are also *not* characteristic ($Z_s = 2.92, p \leq 0.002$, *effect size* = 0.924). Therefore, there appears to be some statistical anomaly associated with the RMS phase shifts for both stimuli types.

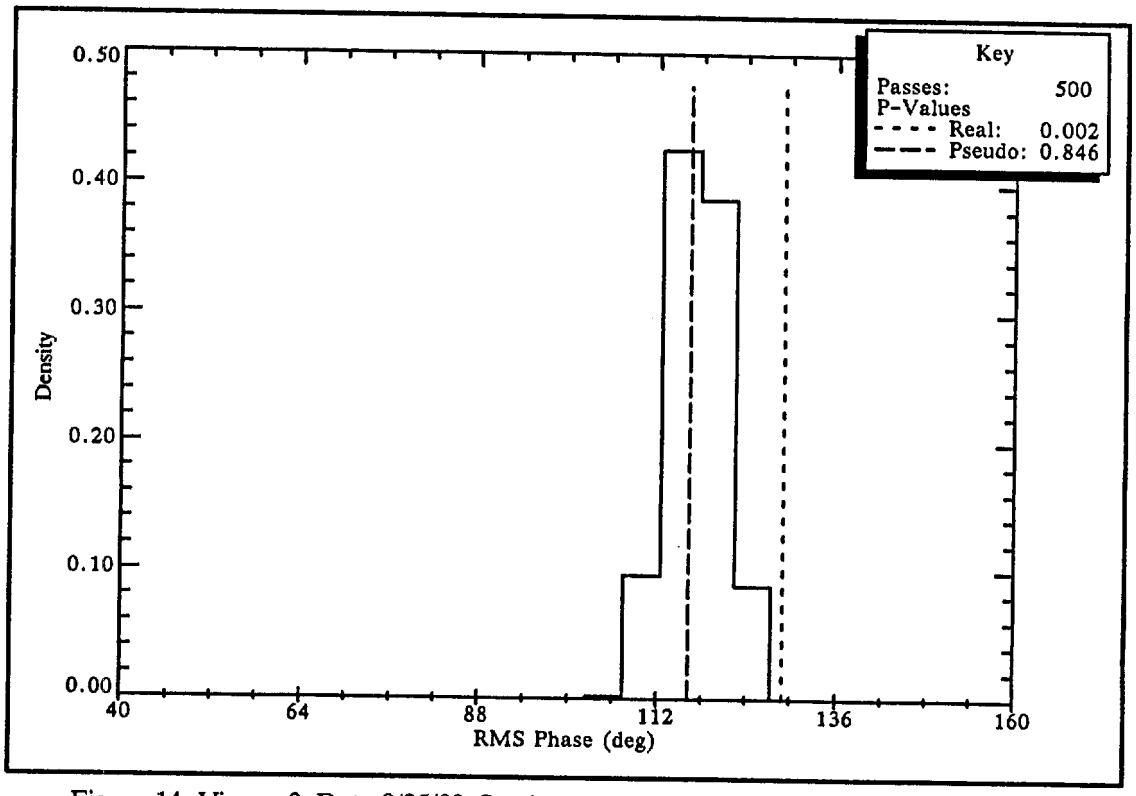

Figure 14 Viewer 2: Date 8/25/88: Session 1: RMS Phase: Sensor: 2: RS = 118

Table 1

Results of Monte Carlo Calculation for RMS Phase

I.D.	Date	Sensor	P-Value (1-tail)		Z-Score (2-tail)	
			Remote	Pseudo	Remote	Pseudo
009	06/24/88	6	0.650	–	–0.524	–
002	08/25/88	2	0.002	0.848	2.653	0.513
	08/26/88	6	0.904	0.966	0.871	1.491
372	10/19/88	7	0.094	0.168	0.885	0.423
374	03/29/89	6	0.154	0.810	0.501	0.305
007	03/29/89	7	0.970	0.180	1.555	0.358
389	05/23/89	4	0.288	0.040	–0.191	1.405
	05/24/89	5	0.260	0.016	–0.050	1.852
	05/25/89	4	0.120	0.922	0.706	1.011
531	05/24/89	4	0.814	0.134	0.274	0.619
454	05/25/89	4	0.732	0.052	–0.090	1.259

3. Results: Button Presses

In the early SRI study[6], significant changes in alpha production were observed in response to an RS. The statistical evidence, however, did not indicate that the viewer was able to recognize an RS cognitively (i.e., the viewer's button presses relative to the RS did not exceed mean chance expectation).

In the current experiment, viewers 002, 009, and 372 were asked to press a button whenever they "perceived" an RS. The total number of stimuli during a session of 10 runs was not known in advance because of the randomization procedure. The null hypothesis is that the probability of a time interval having a stimulus is the same for those intervals with a button press as for those without a button press. In other words, the presence or absence of a stimulus is independent of the presence or absence of a button press. We tested this null hypothesis to determine if a viewer is cognitively aware of the RS.

In Table 2, the fractional hitting rate is $p_1 = A/(A+B)$, and the fractional missing rate is $p_2 = C/(C+D)$. The total number of 1-second intervals is $N = (A+B+C+D)$, and the total stimulus rate is $p_0 = (A+C)/N$.

Table 2

Data Schema for Interval Conditions

		Stimulus	
		Yes	No
Response	Yes	A	B
	No	C	D

Then, under the null hypothesis, the following statistic is approximately normally distributed with a mean of 0 and a variance of 1:

$$z = \frac{(p_1 - p_2)}{\sqrt{p_0(1-p_0)\left(\frac{1}{(A+B)} + \frac{1}{(C+D)}\right)}}.$$

Table 3 shows N, p_0, p_1, p_2, z, p–value, and the effect size, r, for the three sessions for which button-press data were collected. As in the earlier SRI study, there is no indication that the viewers were cognitively aware of the RS.

Table 3

Button Pressing Results

Viewer	N	p_0	p_1	p_2	z	p	r
002	1210	0.167	0.198	0.164	0.951	0.163	0.027
009	1280	0.091	0.068	0.094	–0.978	0.836	–0.027
372	1089	0.157	0.119	0.160	–0.996	0.840	–0.030

IV DISCUSSION AND CONCLUSIONS

We have found statistical evidence that the relative phase shift from -0.5 to 0.5 seconds of an RS are *not* characteristic of the data at large (Z_s = *1.99, p ≤ 0.024, effect size = 0.599*). The combined statistic for the PS indicates that the relative phase shift from -0.5 to 0.5 seconds of a PS are also *not* characteristic of the data at large (*Zs = 2.92, p ≤ 0.002, effect size = 0.924*). Averaged across all viewers, the magnitude of the results, as indicated by their effect sizes of 0.599 and 0.924, respectively, is considered robust by accepted behavioral criteria defined by Cohen.[9*]

1. Root-Mean-Square Phase

Searching for a change of phase as a result of an RS is a natural extension of results quoted in the literature. For example, Rebert and Turner[5] report an example of photic driving (i.e., an extreme example of phase locking) at 16 Hz. In their work, a subject was exposed to a 16-Hz visual DS randomly balanced with no stimulus during 4-second epochs. The average power spectra showed approximately 10-Hz alpha activity during the no-light epochs, and a strong 16-Hz and no 10-Hz peak during the 16-Hz epochs.

One interpretation of their result is that the alpha rhythm was blocked, and the CNS "locked" on to the flashing stimulus. Eason, Oden, White and White,[10] report a phase-shift phenomenon when a rare stimulus, which is random relative to the internal alpha activity, is presented as a DS:

> *"...when a stimulus flash is presented, the resulting primary evoked response acts as a trigger stimulus which temporarily synchronized a certain percentage of the neural elements normally under the influence of an internal pacemaker. ... Desynchronization of the elements participating in the evoked response would occur as the elements are brought back under the influence of an internal pacemaker or are affected by neurons not involved in the response."*

In other words, the internal alpha is momentarily interrupted by an external stimulus, and, in the absence of continuing external stimuli, returns back to its original frequency, but at a random phase relative to its pre-stimulus state.

To understand what would be expected in our experiment for the distribution of RMS phases during the Monte Carlo simulations, we examine a hypothetical case. Suppose that the viewer's alpha activity was a continuous wave at a single frequency. A phase change is computed between 500 ms before and 500 ms after each Monte Carlo "stimulus." Therefore, regardless of the entry point, the relative phase change would be zero, and the RMS phase over many such "stimuli" would also be zero.

Real alpha activity, however, is not continuous, Rather, it appears in bursts lasting from 100 to 5000 ms. Random Monte Carlo "stimuli" would sometimes occur within such bursts and sometimes near the edges. Thus, we would expect a nonzero RMS phase over many such "stimuli," but the individual relative phases would not be uniformly distributed. Depending upon the viewers' alpha characteristics, the distributions would be enhanced near zero RMS phase.

If we assume that Eason, et al., are correct, and that a phase shift is expected as a result of an RS, then the expected distribution of RMS phases is uniformly distributed on $[-\pi, \pi]$. In this case, the phase change is related to the relative timing between the external stimulus and the internal alpha—a completely random relationship. Thus, the variance of the RMS phases in the experimental condition should be larger than those computed during the Monte Carlo runs. Figure 15 is a schematic representation of these models.

* Values of 0.1, 0.3, and 0.5 correspond to small, medium, and large effects, respectively.

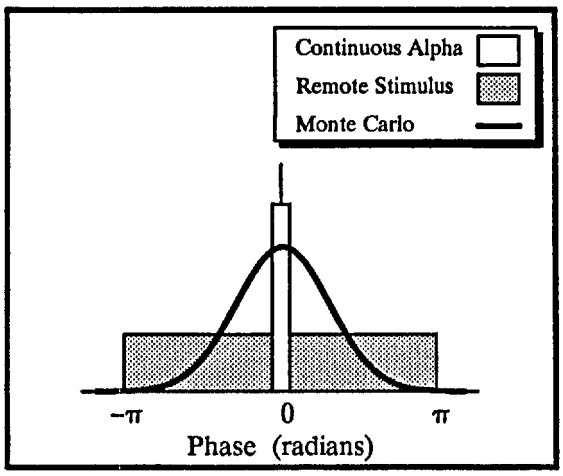

Figure 15 Idealized Distributions for Relative Phase Shifts

As a first step in testing these models, we computed the expected variance for the RMS phase, given that the individual phases are uniformly distributed on [π, π]. Using a Taylor Series expansion for RMS phase, the variance is given by:[11*]

$$\sigma_y^2 = \frac{\frac{3}{45}\pi^2}{n}\left[1 - \frac{1}{30n}\right] \quad (rad^2) \quad , \text{ or}$$

$$\approx \frac{2160}{n} \quad (\deg^2),$$

where n is the number of individual phases.

Table 4 shows the viewer identification, the two-tailed z-score from Table 1, the number of RS, the theoretical variance for the RMS phase, the observed variance from the Monte Carlo runs of 500 passes each, and the X^2 and its associated p-value for a variance-ratio test.

Combining the X^2 across all 11 sessions gives an overall significant result ($X^2 = 5121.5, df = 5489, p \leq 0.0002$). This indicates that the Monte-Carlo-derived variances are significantly smaller than the theoretical variances based on uniformly distributed phases. The two viewers who demonstrated the largest z-scores (002 and 007) also show sharply reduced Monte Carlo variances.

Table 4

Comparison Between Monte Carlo Phases and Theory

I.D.	Z-Score (RS)	Number of RS	Variance of RMS Phase		X^2 df = 499	P-Value
			Theoretical	Observed		
009	-0.524	96	22.50	25.46	564.6	0.978
002	2.653	118	18.31	13.63	371.5	4.9×10^{-6}
	0.871	76	28.42	24.43	428.1	0.010
372	0.885	90	24.00	23.25	483.4	0.316
374	0.501	102	21.18	18.64	439.2	0.025
007	1.555	93	23.23	18.66	400.8	4.6×10^{-4}
389	-0.191	97	22.27	23.35	523.2	0.780
	-0.050	92	23.48	22.29	473/7	0.214
	0.706	98	22.04	20.22	457.8	0.093
531	0.274	101	21.39	21.05	491.1	0.408
454	-0.090	52	41.54	40.48	487.3	0.363

We must conclude that a uniform distribution for the phase is not a good assumption. To determine what the phase distribution was for the RS, we constructed histograms from the raw data.

Figure 16 shows the distribution of phases for the RS and Monte Carlo stimuli for viewer 002. While the RS distribution is enhanced near $\pm$180 degrees and suppressed near 0 degrees compared to the Monte Carlo distribution, the differences are small ($X^2 = 10.62, df = 8, p \leq 0.224$) and, therefore, the random-phase model does not appear to be a good fit to the data for viewer 002 on his 25 September session.

Figure 17 shows the same distributions for viewer 007. In this case, the RS distribution is nearly uniform on [-180,180] degrees, but it differs only

* We thank Professor Jessica M. Utts, Statistics Department, University of California, Davis, California, for suggesting this approach.

slightly from the Monte Carlo distribution ($X^2 = 9.47, df = 8, p \leq 0.304$).

From the data shown in Table 4, we see that the X^2 indicates significant overall differences between the theoretical and observed phase distributions. However, Figures 16 and 17 show that the differences between RS and Monte Carlo distributions are small. It is most probable, therefore, that the RS coupling to the CNS is weak, in general, and that the position of the sensor array is not necessarily optimized to sense the phase changes.

2. Viewer Dependencies

Viewers 002, 009, and 372 have produced consistent remote viewing results for many years—since 1972 for viewers 002 and 009, and since 1979 for viewer 372. Viewer 389 is a recent addition, and has produced examples of excellent remote viewing in the only experiment in which he has participated; however, he has produced significant results in another laboratory. Whereas viewer 002 produced the largest z-score ($Z_s = 2.653$), viewer 009 produced the smallest ($Z_s = -0.524$). The combined effect size for the experienced viewers is 0.621, and is 0.559 for the inexperienced viewers. The difference is not significant.

There are two considerations that prevent drawing conclusions about the viewer dependence of the data. The number of independent samples is small, but the most compelling argument against drawing conclusions is that placement of the sensor array is a seriously confounding factor. As stated in Section II.2, we positioned the array in a location that maximized the response to a DS. This may not be the appropriate positioning for everyone. Indeed, it might not be optimal for anyone.

To determine if there were any "obvious" spatial dependencies that might indicate a more optimal array placement, we computed a complete set (all sensors) of Monte Carlo distributions for one session for viewer 002. Figure 18 shows the single-tailed p-values for the RMS phases for the RS and PS. They are displayed in the standard sensor-array configuration. The pattern for the RS suggests that a more optimal positioning of the array would be in the sensor 2-7 direction as indicated by an arrow in Figure 18.

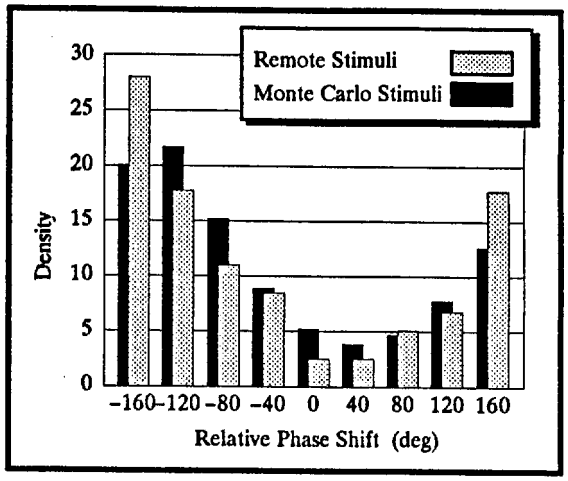

Figure 16 Phase Distributions for Viewer 002: 8/25/88

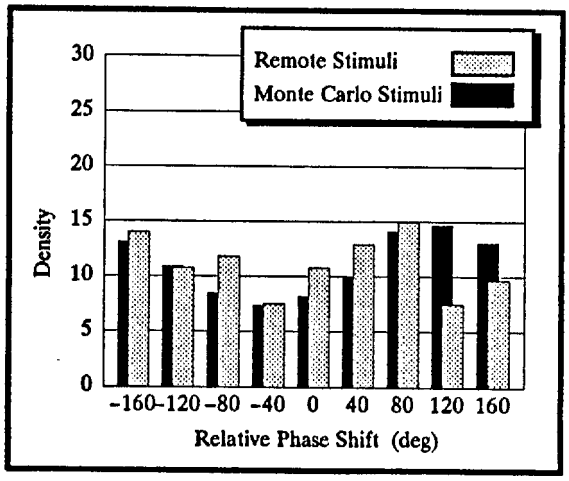

Figure 17 Phase Distributions for Viewer 007: 3/29/89

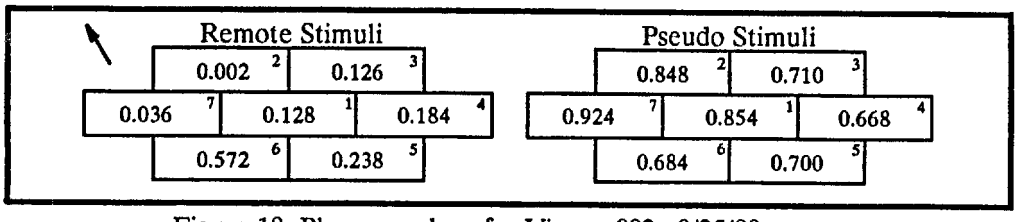

Figure 18 Phase p-values for Viewer 002: 8/25/88

3. Pseudo Stimuli

It was initially thought that the PS would act as a within-run control. The results indicate, however, that there was, on the average, a larger response to the PS than to the RS. While the difference was not significant, it is important to note that both of the responses are considered statistically robust (effect sizes of 0.599 and 0.924 for the RS and PS, respectively). A number of viewers' responses appear to produce phases on opposite sides of the Monte Carlo distributions (e.g., viewers 002 and 007), but there is no overall correlation between the RS and PS p-values.

A brief description of the hardware and software that is responsible for stimulus generation may help in understanding this outcome. The stimuli and their timing are imitated by an HP computer, but are controlled by an IBM PC. Each stimulus type has its own frame buffer within the PC. Our RS consists of a pattern of 1s and 0s that represent a sinusoidal grating in the center of an otherwise blank field. The PS pattern, a blank field that consists of all 0s, resides in a separate buffer. An interface board between the PC and a standard video monitor has its own internal frame buffer, which is automatically and continuously scanned at 30 Hz to provide a standard interleaved video signal. See Figure 19.

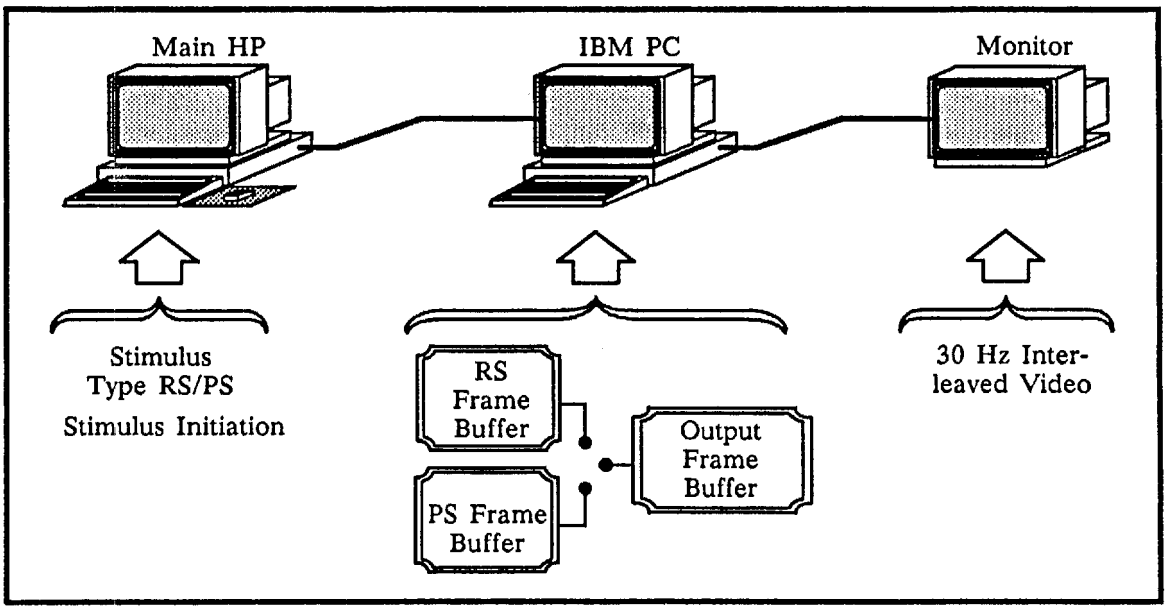

Figure 19 Sequence of Events for Stimuli Generation

When the HP computer signals the PC to provide the appropriate stimulus, the following sequence of events are followed (see Figure 19):

(1) Phase locked to 60 Hz, the interface frame buffer is loaded with a copy of the appropriate stimulus frame buffer (either RS or PS).

(2) The interface board automatically sends this pattern interleaved at 30-Hz.

(3) After a preset time, approximately 100-ms in our experiment, the PC resets the interface frame buffer to zero (blank screen), and waits until another stimulus signal is received.

At the video monitor, the PS are indistinguishable from the between-stimuli blank screens. At the PC, however, the PS are distinguishable from the blank screen background, because the PC must copy a frame buffer (albeit all 0s) into the output frame buffer.

In our experiment, the RS and PS results were statistically identical, and independently, both were significantly different from the Monte Carlo distributions. This raises the question as to what constitutes the target stimulus. Our result is unexpected given the target was considered to be what was displayed on the remote monitor.

It is conceivable that the internal activity of the PC, or its companion computer, was acting as an unintended target. If this were true, then there might be an electromagnetic (EM) coupling between the viewer's CNS and the internal electronic activity of the computers. It is well known

that computers radiate EM energies at relatively high frequencies; for frequencies above 100 Hz, the shielded room is transparent. Analysis of the background runs (i.e., data collected in the absence of a sender or viewer) showed no EM coupling into the MEG electronics; therefore, it remains possible that the statistical effects we have seen are due to CNS responses to remote bursts of EM energy.

Let us *assume* that the overall RS and PS effects are meaningful. Since the PSs are *indistinguishable* at the monitor from the between-stimuli background but are *distinguishable* at the IBM PC, then the present experiment demonstrates that the source of stimuli is the IBM PC.

During the SRI/Langley Porter study in 1977, SRI developed an entirely battery operated stimulus generator as a special precaution against the possibility of system artifacts in the form of EM pickup. They reported significant CNS responses to remote stimuli, nonetheless.[6] Therefore, it remains possible that we have observed an anomalous information transfer.

Before further research is conducted, it is important to measure the EM radiation, and to see if it is of sufficient strength to be detected (by the appropriate hardware) in the shielded room.

By adjusting the PC program, the PS internal activity can be eliminated. It would be interesting to see if the similarity between the RS and PS results persists.

REFERENCES

1. Dean, E. D., *International Journal of Neuropsychiatry,* Vol. 2, p 439, 1966.
2. Tart, C. T., *International Journal of Parapsychology,* Vol. 5, p 375, 1963.
3. Duane, T. D., and Behrendt, T., *Science,* Vol. 150, p. 367, 1965.
4. Cavanna, R., Ed., *Psi Favorable States of Consciousness,* Parapsychology Foundation, New York, 1970.
5. Rebert, C. S., and Turner, A., "EEG Spectrum Analysis Techniques Applied to the Problem of Psi Phenomena," *Physician's Drug Manual,* Vol. 6, Nos. 1-8, pp 82-88, 1974.
6. Targ, R., May, E. C., Puthoff, H. E., Galin, D., and Ornstein, R., "Sensing of Remote EM Sources (Physiological Correlates)," Final Report, Project 4540, SRI International, Menlo Park, CA, 1977.
7. Sutherling, W. W., Crandall, P. H., Cahan, L. D., and Barth, D. S., "The Magnetic Field of Epileptic Spikes Agrees with Intracranial Localizations in Complex Partial Epilepsy," *Neurology,* Vol. 38, No. 5, pp 778-786, May 1988.
8. Aine, C. J., George, J. S., Medvick, P. A., Oakley, M. T., and Flynn, E. R., "Source Localization of Components of the Visual-Evoked Neuromagnetic Response," Neuromagnetism Laboratory, Life Sciences and Physics Divisions, Los Alamos National Laboratory, Los Alamos, NM.
9. Cohen, J., *Statistical Power Analysis for the Behavioral Sciences* (rev. ed.), Academic Press, New York, 1977.
10. Eason, R. G., Oden, D., White, B. A., and White, C. T., "Visually Evoked Cortical Potentials and Reaction Time in Relation to Site of Retinal Stimulation," *Electroencephalography and Clinical Neurophysiology,* Vol. 22, pp 313-324, 1967.
11. Rice, J. A., *Mathematical Statistics and Data Analysis,* Wadsworth & Brooks/Cole Advanced Books & Software, Pacific Grove, p 143, 1988.